JOC The Journal of Organic Chemistry

pubs.acs.org/joc Article

Octapodal Corannulene Porphyrin-Based Assemblies: Allosteric Behavior in Fullerene Hosting

Sergio Ferrero, Héctor Barbero, Daniel Miguel, Raúl García-Rodríguez,* and Celedonio M. Álvarez*

Cite This: J. Org. Chem. 2020, 85, 4918−4926 Read Online

ACCESS | Metrics & More | Article Recommendations | Supporting Information

ABSTRACT: An octapodal corannulene-based supramolecular system has been prepared by introducing eight corannulene moieties in a porphyrin scaffold. Despite the potential of this double picket fence porphyrin for double-tweezer behavior, NMR titrations show exclusive formation of 1:1 adducts. The system exhibits very strong affinity for C_{60} and C_{70} (K_1 = (2.71 ± 0.08) × 10^4 and (2.13 ± 0.1) × 10^5 M^{-1}, respectively), presenting selectivity for the latter. Density functional theory (DFT) calculations indicate that, in addition to the four corannulene units, the relatively flexible porphyrin tether actively participates in the recognition process, resulting in a strong synergistic effect. This leads to a very strong interaction with C_{60}, which in turn also induces a large structural change on the other face (second potential binding site), leading to a negative allosteric effect. We also introduced Zn^{2+} in the porphyrin core in an attempt to modulate its flexibility. The resulting metalloporphyrin also displayed single-tweezer behavior, albeit with slightly smaller binding constants for C_{60} and C_{70}, suggesting that the effect of the coordination of fullerene to one face of our supramolecular platform was still transmitted to the other face, leading to the deactivation of the second potential binding site.

INTRODUCTION

Since its establishment, supramolecular chemistry[1] has been used to design and develop new entities with a wide range of applications in various areas of science. Inspired by nature, an interesting topic in supramolecular chemistry is the development of artificial receptors that echo the allosteric control of more complex biological systems.[2] The term allosterism describes structural changes that occur upon the coordination of a substrate to a binding site (allosteric site) of the host.[3] The information associated with the first event is transmitted to a different binding site by a change in the conformation, which can lead to activation (positive cooperation) or deactivation (negative cooperation or inhibition) of the binding site. This represents a very useful tool to control the coordination of different sites, and not surprisingly, it has attracted a great deal of attention in the supramolecular chemistry community.[4]

Additionally, carbon nanostructures, particularly fullerenes, have found a variety of applications in supramolecular chemistry due to their unique structures and electronic properties.[5] Great efforts have been made to construct supramolecular assemblies that host fullerenes through weak intermolecular forces[6] to develop high-performance devices, in particular, photoelectrochemical devices and solar cells.

Size and shape complementarity is crucial to achieving efficient supramolecular host−guest binding. In this regard, bowl-shaped aromatic hydrocarbons or buckybowls[7] are attracting increasing attention and finding new applications in materials science.[8] Corannulene,[9] the most-interesting buckybowl, has unique properties not seen in planar π-conjugated compounds arising from its nonplanarity, which enables it to form supramolecular assemblies with fullerenes through noncovalent interactions. Its net dipolar moment,[10] together with its exceptional concave−convex complementary for π−π stacking,[11] allows it to strongly interact with fullerenes via the well-known "ball-and-socket" interactions. Not surprisingly, corannulene has proven to be a very useful motif for the design of various materials and a very attractive building block in the construction of organic electronic devices, including solar cells and nonlinear optical materials.[8b,12] In particular, it has played a central role in the design of efficient receptors for fullerenes. The use of corannulene as a building block, however, has been limited by its tedious synthesis, which requires a large number of steps. Considerable efforts have been devoted to improving the current synthetic methods as well as to its derivatization with suitable functional groups to enable its use in producing more complex architectures. Although a single pristine corannulene unit cannot bind fullerene strongly enough for the corannulene−

Received: January 10, 2020
Published: March 10, 2020

https://dx.doi.org/10.1021/acs.joc.0c00072
J. Org. Chem. 2020, 85, 4918−4926

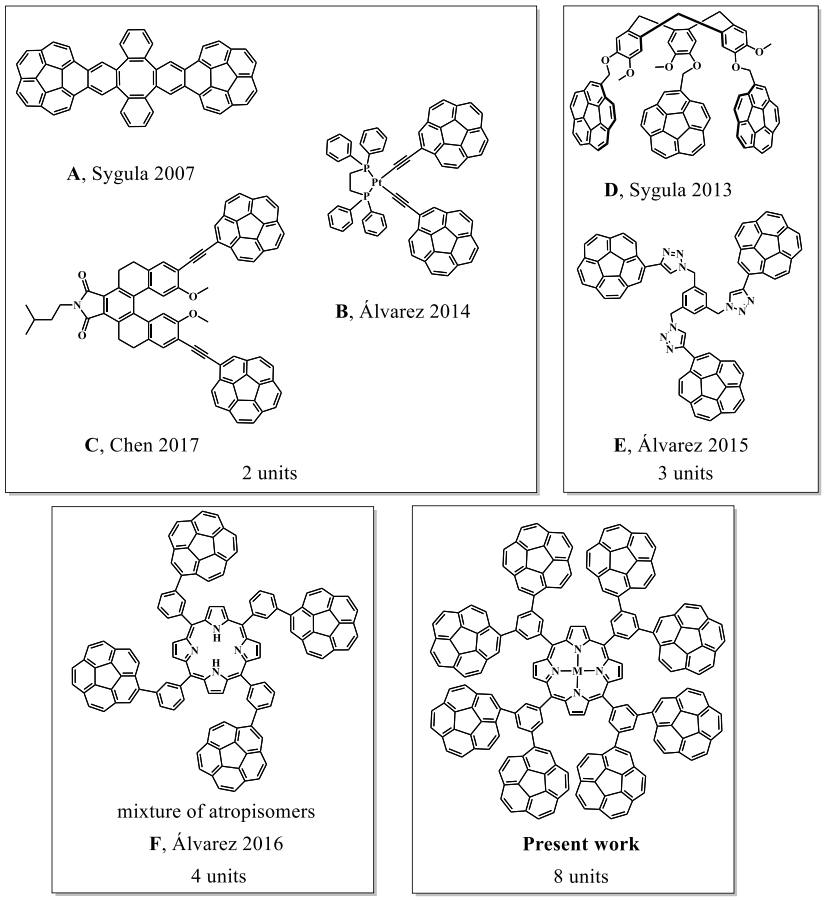

Figure 1. Development of systems bearing different numbers of corannulene units.

fullerene inclusion complex to be observed in solution,[13] the careful design of molecules incorporating two corannulene units has proven to be a very useful strategy to improve corannulene−fullerene interactions.

Researchers have long focused on improving the strength and selectivity of fullerene receptors. The historical evolution of multicorannulene "pincer" systems is shown in Figure 1, which shows selected examples. The first and most obvious such pincer systems were based on two corannulene units and have had a great impact on supramolecular−fullerene interactions. In particular, Sygula's buckycatcher I (Figure 1, A)[14] represented a breakthrough as the first example of the formation of a stable inclusion complex with fullerene and presented association constants of 2.78×10^3 M^{-1} (C_{60}) and 3.03×10^3 M^{-1} (C_{70}) in toluene at 298 K. Sygula subsequently engineered the tether between the two corannulene moieties to improve the preorganization of the host and the fullerene guest, expanding the buckycatcher family (buckycatchers II and III, not depicted in the figure)[15] and improving the C_{60} binding constant by an order of magnitude. We developed a platinum-based system with two corannulene moieties, which was the first system capable of discriminating C_{60} over C_{70} (B); subsequently, Chen et al. achieved outstanding discrimination ($K_{C_{70}}/K_{C_{60}}$ = 230:1) using the two-corannulene moiety system C.[16] In contrast, systems bearing tris-corannulene clips,[17] such as D and E, have not had the same success as systems bearing two corannulene units due to their lower ability to associate fullerenes. The lower binding constants observed for these tripodal systems ($K_1 = 1.50 \times 10^3$ M^{-1} (C_{60}) and $K_1 = 2.19 \times 10^3$ M^{-1} (C_{60}) for D and E systems, respectively) seem to stem from their much greater flexibility, which favors self-interaction and consequently notably reduces their interaction with fullerenes. These examples highlight the importance of the preorganization and morphology of the supramolecular platform in fullerene association, which can be as important as the number of corannulene units attached. Therefore, to increase host−guest surface contact, careful design of fullerene receptors is required in addition to increasing the number of corannulene units.[18]

We have recently explored the use of porphyrin-based systems as molecular scaffolds for fullerene hosting. Although porphyrins and fullerenes can interact, the presence of only a single porphyrin core usually results in interactions with fullerenes that are too weak to be observed in solution.[19] These systems are relatively rigid and allow for the active participation of the tether in the supramolecular interaction and are therefore ideally suited to host fullerenes. We envisaged that a meso-substituted tetraaryl porphyrin core would be an ideal scaffold for supramolecular interactions and prepared the meta-substituted porphyrin F with four corannulene units.[18b] However, while this tetrakis-corannulene porphyrin clip was able to associate with C_{60}, F was present as a difficult-to-analyze mixture of four atropisomers resulting from the orientation of the four corannulene units above and below the porphyrin plane. These atropisomers could not be separated, resulting in a complex system and marked decrease in the C_{60} binding ability. In a recent work, we subsequently circumvented the formation of atropisomers by introducing eight pyrene units at the meta positions of the tetraaryl

https://dx.doi.org/10.1021/acs.joc.0c00072
J. Org. Chem. 2020, 85, 4918−4926

porphyrin system.[20] This resulted in a double tweezer with a remarkably high association for fullerenes, despite the poor shape complementarity between pyrene and fullerenes, due to the synergistic effect between the porphyrin tether and the pyrene units. As the combination of well-organized corannulene fragments and a porphyrin tether resulted in synergistic effects and good fullerene hosting ability, in the present work, we explore the possibility of introducing eight corannulene units on a single porphyrin core (Figure 1, present work) and their impact on the fullerene affinity and selectivity of the new octapodal corannulene supramolecular platform (which contains the most corannulene moieties on a single-molecule receptor to date). The effect of the association on the geometry of the double tweezer (allosteric effect) and its impact on a second association event, which determines whether the receptor will exhibit double- or single-tweezer behavior, are studied. This is an important issue since the development of artificial and well-defined systems in which allosteric effects can control the association behavior, echoing more complex biological systems, is a great challenge.

RESULTS AND DISCUSSION

To obtain the octapodal corannulene target compound, we employed a "corannulene LEGO brick" approach using a divergent synthesis in which a suitable porphyrin-based scaffold is first prepared to further allow the introduction of eight corannulene units. The meta-substituted octabromoporphyrin **2H-POctaBr** was selected as an ideal starting porphyrin core from which further elaboration of the porphyrin framework could be accomplished. **2H-POctaBr** presents eight bromine atoms in the meta positions of the tetraaryl meso-substituted porphyrin (Scheme 1a) and therefore could be used in the palladium-catalyzed Suzuki reaction with the appropriate boronic ester of corannulene. Synthesis of **2H-POctaBr** was accomplished using our previously reported microwave-assisted method.[20] We next prepared 1-pinacol corannuleneboronate (**BPin-Cor**), which is the key "LEGO" fragment for the introduction of corannulene to the system via Suzuki reactions at the eight bromines of **2H-POctaBr**. The borylation of corannulene to furnish **Bpin-Cor** was accomplished from 1-bromocorannulene (**Br-Cor**) via a microwave-assisted Miyaura reaction in just 80 min (Scheme 1b), which represented a significant improvement over the routine benchtop preparation (typically 24 h reflux in dioxane). Subsequently, the Suzuki reactions of **2H-POctaBr** and **Bpin-Cor** were accomplished via an MW-assisted octuple Suzuki reaction (150 °C, 135 min, toluene) (Scheme 1c). In this manner, compound **2H-POctaCor** was isolated in 15% total yield after optimization, which we considered quite satisfactory given the eight reactions involved. The use of an MW reactor has been reported to be crucial in multiple C−C coupling reactions in which the rapid buildup of byproducts might hinder product formation.[21] Indeed, changing the cross-coupling partners in the Suzuki reaction (i.e., Br-corannulene and octaborylated porphyrin) led to a disappointing 3% yield. In this case, a range of impurities and incomplete reaction products (containing less than eight corannulene moieties) prevented us from obtaining **2H-POctaCor** in the pure form.

Despite its low solubility, the octapodal corannulene porphyrin **2H-POctaCor** was characterized by spectroscopic methods (see the Experimental Section). Further confirmation of the formation of **2H-POctaCor** was provided by high-resolution mass spectrometry, which showed the expected [M + H]$^+$ peak at m/z 2601.7586 (calcd 2601.7619; see the Supporting Information, Figure S24). The UV−vis absorption spectra show the typical intense Soret band at 426 nm, and the ^{1}H NMR spectrum of **2H-POctaCor** in chloroform-d was remarkably simple due to the highly symmetrical nature of the compound. A characteristic upfield signal for the porphyrin NH protons is observed at $\delta = -2.50$ ppm. Only one β pyrrole proton resonance was observed, which, along with the equivalence of the eight corannulene moieties, indicated an effective D_{4h} symmetry in solution. Notably, the ^{1}H NMR signals are markedly broad and do not change significantly upon dilution (see the Supporting Information, Figure S2). Although a certain degree of intermolecular $\pi-\pi$ stacking is likely, this suggests that intramolecular $\pi-\pi$ interactions could also be occurring.[17a,22]

Scheme 1. Synthesis of 2H-POctaCor[a]

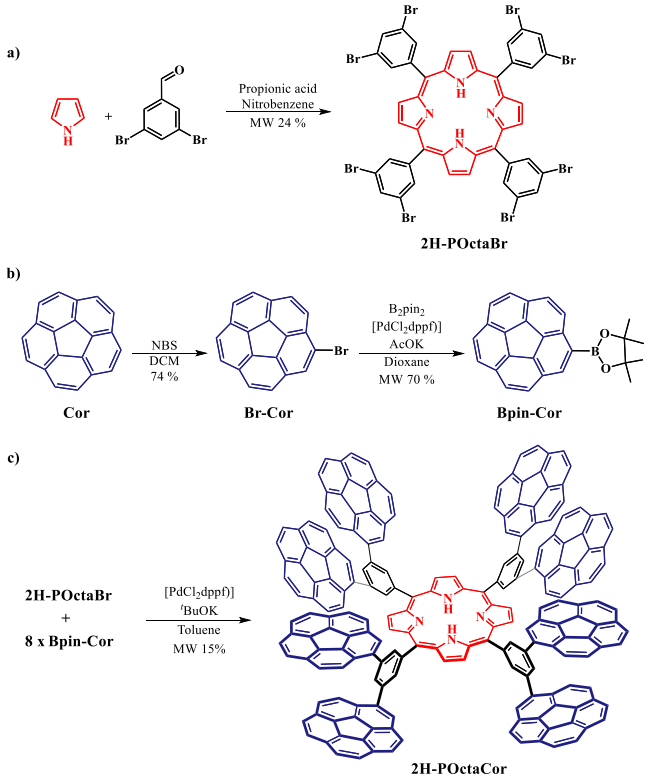

[a]Yields of every step are included.

To further explore this possibility, compound **2H-POctaCor** was first optimized using a conformational screening by molecular mechanics and, subsequently, full DFT optimization of the best candidates at the B97D3/6-31G(d,p) level of theory[23] (see the Supporting Information for details). Interestingly, the lowest energy minimum corresponds to a conformer whose porphyrin core has been substantially distorted, giving rise to a saddlelike geometry (Figure 2). This situation stems from the highly attractive concave−convex stacking interactions between pairs of corannulene groups. The potential formation of conformers resulting from these interactions likely contributes to the broadening of the signals observed in the ^{1}H NMR spectrum. Figure 2a shows that $\pi-\pi$ interactions are established between pairs of corannulenes, leading to a 4 + 4 arrangement of the corannulene units below and above the distorted porphyrin plane in a "double picket fence" arrangement. This type of

https://dx.doi.org/10.1021/acs.joc.0c00072
J. Org. Chem. 2020, 85, 4918−4926

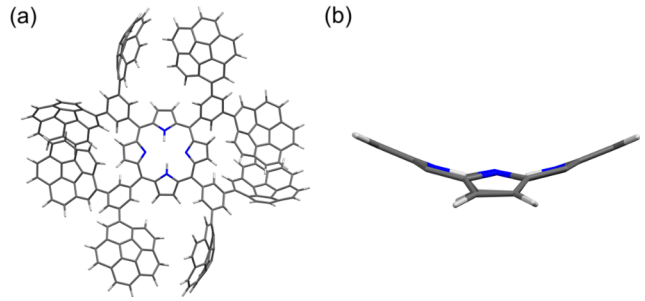

Figure 2. (a) Top view of the lowest energy minimum optimized structure of compound **2H-POctaCor** and (b) side view of the porphyrin core.

arrangement could potentially lead to the binding of two fullerenes. However, such corannulene $\pi-\pi$ interactions could conceivably produce a potential energy penalty for the adoption of an optimal structure for fullerene hosting by the molecule, as all of the corannulene interactions must be overcome beforehand.

To investigate these potential issues and study the supramolecular behavior and fullerene hosting ability of **2H-POctaCor**, we carried out titration experiments with C_{60} and C_{70} in toluene-d_8. One particular facet we were interested in exploring was whether our octapodal corannulene-based system could allow the binding of two fullerenes (see idealized Scheme 1c). Due to the low solubility of **2H-POctaCor**, a host concentration of $[H]_0 = 10^{-5}$ M was selected. Upon the addition of 0.17 equiv of C_{60}, a shift in the ^{1}H NMR signals was observed, indicating supramolecular association between **2H-POctaCor** and C_{60}. This shift was initially accompanied by further broadening of the signals (Figure 3 above). This was attributed to an intermediate-exchange regime[24] between the free and bound guests on the NMR time scale, which is supported by the fact that toward the end of the titration (in the presence of an excess of C_{60}), the signals again became sharper, since the equilibrium was then completely shifted toward the formation of the C_{60}**@2H-POctaCor** complex. The β pyrrole proton resonance, which remained relatively sharp and well-defined throughout the process, was found to be a convenient signal to follow the titration (Figure 3 above).

Similar behavior was observed in the titration of **2H-POctaCor** and C_{70} (Figure 3 below). Upon the addition of C_{70}, a shift in the signals indicative of host–guest formation was observed, although in this case, much greater concomitant broadening of the signals was produced. Despite this, the β pyrrole proton resonance could still be used as a good probe to follow the process (Figure 3 below). For both titration experiments, the nonlinear binding isotherms obtained could be fitted to a 1:1 model (Figure 3, insets). The calculated binding constant for C_{70} ($K_1 = (2.13 \pm 0.10) \times 10^5$ M^{-1}) was 1 order of magnitude larger than that of C_{60} ($K_1 = (2.71 \pm 0.08) \times 10^4$ M^{-1}). This shows that our supramolecular platform exhibits a certain degree of selectivity for C_{70} and that the interactions among the corannulene moieties in the absence of fullerene (Figure 2) do not apparently diminish its fullerene hosting ability. This is in contrast to the more flexible tris-corannulene systems **D** or **E** in Figure 1, for which these interactions resulted in very low affinities for C_{60}. Importantly, despite the obvious potential of our octapodal corannulene system to act as a double tweezer (Scheme 1c), no evidence for a 1:2 model was observed. As noted in the

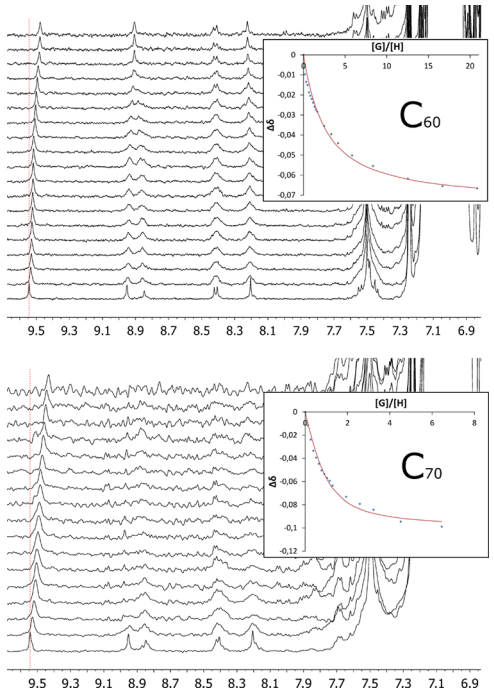

Figure 3. ^{1}H NMR spectra (500 MHz, toluene-d_8) showing the chemical shift of the H_2 proton of **2H-PoctaCor** upon the addition of aliquots of C_{60} (above) or C_{70} (below). Insets: Plots of the changes in the chemical shift against [G]/[H], where G is C_{60} or C_{70} and H is **2H-PoctaCor**. The red line corresponds to the nonlinear fitting of $\Delta\delta$ for H_2 to a 1:1 binding isotherm. Note: The dotted red line over the spectrum is a guide for the eye.

Introduction, cooperative effects are a key aspect for understanding recognition processes in supramolecular chemistry and play a central role in complex biological systems (i.e., in the recognition processes of proteins such as allosteric control). Both positive and negative cooperation (inhibition) effects play very important roles in biological systems. A well-known example of the latter is the coordination of cytidine triphosphate to the enzyme aspartate-transcarbamoylase, which induces a conformational change that produces an inactive conformation.[25] Another iconic example is the coordination of O_2 to hemoglobin. The coordination of the first molecule of O_2 induces conformational changes that result in a larger binding affinity for the coordination of O_2 to the remaining binding sites.[26]

To obtain further insights into this interesting phenomenon, DFT calculations were performed to determine the mechanism by which 1:1 rather than 1:2 binding stoichiometry was observed and whether all of the corannulene units are involved in the recognition process. Indeed, our octapodal corannulene system is ideally suited to study the possibility of cooperative effects in the fullerene recognition process. The structure of the inclusion complex C_{60}**@2H-POctaCor** obtained by DFT is shown in Figure 4 (see the Supporting Information for details). As can be seen, the porphyrin core has a degree of flexibility; this flexibility not only allows the approach of the four corannulene moieties to C_{60} for an optimal interaction but also allows the core itself to actively participate in the recognition process (see later). The ortho hydrogens of the phenylene substituents tend to point away from the fullerene molecule, maximizing the interaction of the corannulene units with the outer surface of C_{60}. Thus, the structural arrangement is the

https://dx.doi.org/10.1021/acs.joc.0c00072
J. Org. Chem. 2020, 85, 4918–4926

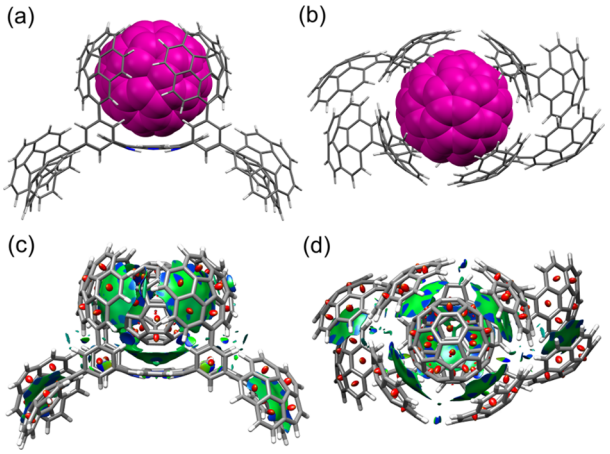

Figure 4. DFT-optimized structure of C_{60}@**2H-PoctaCor**. Side (a) and top (b) views of the optimized structure. Side (c) and top (d) views of NCI plots for the optimized structure of C_{60}@**2H-PoctaCor**.

result of the maximization of supramolecular binding, allowing better complementarity between both surfaces. This can be observed by the fact that all corannulene units on the same face of the porphyrin are arranged for an optimal interaction with the outer surface of the fullerene. Additionally, the contribution of the porphyrin core itself to this interaction is not negligible, as the distance between the core and the fullerene falls within the range of attractive dispersion contacts. These strong interactions lead to the compression of the corannulene arms of the active face of the porphyrin to effectively wrap the C_{60} surface.

The supramolecular bonding interactions between the host and C_{60} are the most clearly illustrated on the basis of critical points.[27] Figure 4c,d shows five bowl-shaped attractive interactions between the fullerene and the molecular clip **2H-PoctaCor**. In addition to the four interactions from the four corannulene arms, an additional interaction with the porphyrin core is clearly observed. This demonstrates the excellent complementarity between C_{60} and our molecular platform, as revealed by the fact that the isosurface almost totally covers the fullerene surface. Additional interactions between the remaining corannulenes on the other face of the molecule are also observed, indicating that the intramolecular interactions among the four remaining corannulenes also contribute to the stabilization of this structural arrangement.

Our data indicate that in the presence of fullerene, an equilibrium is reached between free C_{60} and 1:1 C_{60}@**2H-POctaCor** adducts (K_1). This association deforms the geometry of **2H-POctaCor** in such a way that the second face of the porphyrin cannot effectively bind a second C_{60} fullerene. Figure 4a shows that concomitant to the organization of the active face of the porphyrin around C_{60} (compression), the arms of the other face expand significantly, leading to poor preorganization of the host for interaction with a second fullerene, as the four corannulene units of the inactive face are now too far away from each other to effectively interact with a second C_{60}.

We also explored the effect of a second binding event. The structure of the inclusion complex $(C_{60})_2$@**2H-POctaCor** was optimized by DFT calculations (see the Supporting Information). The data reveals that, as expected, the hosting of one C_{60} in (C_{60})@**2H-POctaCor** hampers the efficient association of a second C_{60}. Indeed, this results in a suboptimal conformation of the receptor, in which the interaction between the first C_{60} and the porphyrin core is greatly reduced to partially cover the second C_{60} (see the Supporting Information for details). The acceptance of the first fullerene, therefore, leads to negative allosteric induction, preventing the binding of a second C_{60}. This effect can be ascribed to the change in the conformation of the second binding face of the receptor upon the coordination of the first fullerene.

Metal coordination is known to lead to changes in the geometry of the porphyrin ring. To study whether the inhibitory conformational change of the current system upon association with a first C_{60} moiety could be prevented, we introduced Zn^{2+} in the porphyrin. The resulting metalloporphyrin, **Zn-POctaCor**, was expected to exhibit a reduced degree of flexibility compared to that of the porphyrin **2H-POctaCor** as a result of metal coordination.

The introduction of a Zn^{2+} in the porphyrin was easily accomplished in a quantitative manner using a microwave-assisted method (see Scheme 2 and the Experimental Section).

Scheme 2. Synthesis of Zn-POctaCor[a]

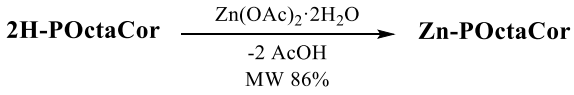

[a]Reagents and conditions: $Zn(OAc)_2{\cdot}2H_2O$, $CHCl_3$/toluene, MW. Yield included.

The ^{1}H NMR spectrum shows the disappearance of the inner 2H porphyrin protons, and the UV−vis spectrum exhibited a small red shift in the Soret band (431 nm) compared to that of **2H-POctaCor** (426 nm), suggesting that metal coordination slightly distorts the planarity of the porphyrin core.[28]

Titration of **Zn-POctaCor** with C_{60} and C_{70} revealed a shift in the signals accompanied with a very large broadening. Although the peak broadening made the analysis challenging, a 1:1 model could be observed in both cases (see the Supporting Information). The calculated binding constants, K_1 = (2.19 ± 0.05) × 10^4 and (1.16 ± 0.40) × 10^5 M^{-1} for C_{60} and C_{70}, respectively, are slightly smaller than those obtained for **2H-POctaCor** and also indicate selectivity for C_{70} over C_{60} (Table 1).

Table 1. Summary of Binding Constants K_1 (M^{-1}) for 2H-POctaCor and Zn-POctaCor for Different Fullerenes in Toluene-d_8

	C_{60}	C_{70}
2H-POctaCor	(2.71 ± 0.08) × 10^4	(2.13 ± 0.10) × 10^5
Zn-POctaCor	(2.19 ± 0.05) × 10^4	(1.16 ± 0.40) × 10^5

These results suggest that although coordination to Zn^{2+} reduced the flexibility of the system somewhat, which in turn led to smaller binding constants, it did not completely prevent the expansion of the other porphyrin face upon the coordination of the fullerene. This structural arrangement would disfavor the coordination of a second fullerene, leading to the formation of the experimentally observed 1:1 fullerene adduct.

CONCLUSIONS

An octapodal corannulene porphyrin-based molecular clip and its Zn-complexed metalloporphyrin analogue have been

https://dx.doi.org/10.1021/acs.joc.0c00072
J. Org. Chem. 2020, 85, 4918−4926

prepared. This new molecular platform contains the largest number of corannulene units reported for a single molecule and shows very strong associations as C_{60} and C_{70} hosts, with larger affinities for the latter, indicating selectivity for C_{70} over C_{60}. Despite the presence of two potential binding sites, the system behaves as a single rather than a double tweezer, leading to the formation of 1:1 adducts with fullerene. DFT calculations indicate that the four corannulene moieties and the porphyrin core participate in the recognition process, resulting in very strong binding of C_{60} and a large conformational change in the molecular clip. This conformational change is transmitted to the second binding site, resulting in the expansion of its cavity and, consequently, its deactivation. The allosteric effects observed in the novel octacorannulene double picket fence porphyrin could enable the accommodation of a larger host (such as a higher-order fullerene) in the expanded second binding site, resulting in a modular supramolecular platform that echoes allosteric regulation in biological systems. Work in our group is underway to study the interplay (compression/expansion) of the two faces to tailor the system for specific host/guest interactions.

EXPERIMENTAL SECTION

General Methods. All reagents were purchased from commercial sources and used without further purification. Solvents were either used as purchased or dried according to procedures described elsewhere.[29] Microwave reactions were carried out on sealed vessels using an Anton Paar Monowave 300 Reactor. Column chromatography was carried out using silica gel 60 (particle size 0.040−0.063 mm; 230−400 mesh) as the stationary phase, and thin layer chromatography (TLC) was performed on precoated silica gel plates (0.25 mm thick, 60 F254) and visualized under UV light and/or by immersion in anisaldehyde. NMR spectra and NMR titrations were recorded on 500 MHz Agilent DD2 instruments equipped with a cold probe in the Laboratory of Instrumental Techniques (LTI) Research Facilities, University of Valladolid. ^{1}H and ^{13}C NMR chemical shifts (δ) are reported in parts per million (ppm) and are referenced to tetramethylsilane (TMS), using the residual solvent peak as an internal reference. Coupling constants (J) are reported in Hz. Standard abbreviations are used to indicate multiplicity: s, singlet; d, doublet; t, triplet; and m, multiplet. ^{1}H and ^{13}C peak assignments were performed using 2D NMR methods (DQFCOSY, band selective ^{1}H−^{1}H-ROESY, band selective ^{1}H−^{13}C HSQC, band selective ^{1}H−^{13}C HMBC). Due to the low solubility, some carbon signals were detected indirectly via ^{1}H−^{13}C-HSQC/HMBC experiments. High-resolution mass spectra were recorded at the mass spectrometry service of the Laboratory of Instrumental Techniques of the (LTI) University of Valladolid. A MALDI-TOF system (MALDI-TOF), the Bruker Autoflex Speed (N_2 laser: 337 nm, pulse energy 100 μJ, 1 ns; acceleration voltage: 19 kV, reflector positive mode), was used. Trans 2-[3-(4-*tert*-butylphenyl)-2-methyl-2-propenylidene]malonitrile (DCTB) and 1,8,9-anthracenetriol, 1,8-dihydroxy-9(10*H*)-anthracenone (dithranol) were used as matrices. UV−vis spectra were recorded using a Shimadzu UV-1603 with spectrophotometric-grade solvents. UV−vis absorption spectral wavelengths (λ) are reported in nanometers (nm), and molar absorption coefficients (ε) are reported in $M^{-1}\cdot cm^{-1}$. Corannulene was obtained following the literature procedures.[9e] Synthesis and characterization of the compound **2H-POctaBr** have been previously reported by our group.[20]

Br-Cor. Corannulene (50 mg, 0.199 mmol) and freshly recrystallized *N*-bromosuccinimide (37.3 mg, 0.209 mmol) were placed into a 5 mL round-bottomed flask and dissolved in 690 μL of dry dichloromethane (DCM). The reaction was monitored using ^{1}H NMR spectroscopy until the corannulene signal disappeared. After stirring the mixture at room temperature (RT) for 21 h, 10 mL of saturated NH_4Cl was added to quench the reaction. The crude was treated with 10 mL of DCM and placed into a separatory funnel. The organic phase was washed with 15 mL of warm H_2O twice, and the aqueous phase was extracted with 10 mL of DCM. The solvent of the organic phase was removed under vacuum, and the crude was purified by column chromatography on silica gel (hexane) to obtain **Br-Cor** (48.4 mg, 74%) as a fluffy yellow solid. The spectroscopic data were in agreement with the data reported in the literature.[9c]

Bpin-Cor. **Br-Cor** (66 mg, 0.200 mmol), bis(pinacolato)diboron (76.18 mg, 0.300 mmol), [$PdCl_2$(dppf)] (7.31 mg, 0.01 mmol), and AcOK (58.57 mg, 0.6 mmol) were mixed into a sealed vessel specifically designed for microwave irradiation and placed into a microwave reactor inside a two-necked round-bottomed flask to maintain the system under an inert atmosphere. Dry dioxane (1.2 mL) was added to the microwave vessel. The mixture was stirred inside the microwave reactor at 165 °C for 80 min; the pressure reached 5.8 bar. Subsequently, the solvent was removed under low pressure, and the crude was purified using column chromatography on silica gel; hexane/AcOEt gradient elution (20:1−15:1−10:1−5:1−3:1−1:1—AcOEt) yielded **Bpin-Cor** (52.5 mg, 70%) as a yellow oil. The spectroscopic data were in agreement with the data reported in the literature.[30]

2H-POctaCor. **2H-POctaBr** (10 mg, 0.0080 mmol), **Bpin-Cor** (26.7 mg, 0.071 mmol), [$PdCl_2$(dppf)] (9.3 mg, 0.0128 mmol), and ^{t}BuONa (18.5 mg, 0.192 mmol) were mixed in a sealed vessel specifically designed for microwave irradiation and placed in a microwave reactor inside a two-necked round-bottomed flask to keep the system under an inert atmosphere. Then, 1.4 mL of dry toluene was added. The mixture was stirred inside the microwave reactor at 150 °C for 135 min; the pressure reached 3.8 bar. After cooling, the solvent was removed under vacuum, and the crude was purified by column chromatography on silica gel using hexane/AcOEt gradient elution (3:1−2:1−1:1) and $CHCl_3$ to finally give a purple solid corresponding to **2H-POctaCor** (3.1 mg, 15%). ^{1}H NMR (500 MHz, chloroform-*d*) δ: 9.31 (s, 8H, H_2), 8.85 (s, 8H, H_6), 8.69 (s, 4H, H_8), 8.35−8.26 (m, 16H, H_{10} + H_{11}), 7.93−7.70 (m, 56H, H_{12} + H_{13} H_{14} + H_{15} + H_{16} + H_{17} + H_{18}), −2.50 (br, 2H, H_1). ^{13}C{^{1}H} NMR (126 MHz, chloroform-*d*) δ: 136.4, 136.2, 135.8, 135.6 (C_6), 135.3, 130.9, 130.8 (C_8), 129.5, 128.1−126.3 (C_{10} + C_{11} + C_{12} + C_{13} + C_{14} + C_{15} + C_{16} + C_{17} + C_{18}). HRMS (MALDI-TOF) *m/z*: $[M + H]^+$ calcd for $C_{204}H_{94}N_4$ 2601.7619; found 2601.7586 (3.3 ppm error). UV−vis (toluene): λ 426 (ε = 279 556), 520 (ε = 12 969), 544 (ε = 7205).

Zn-POctaCor. **2H-POctaCor** (2.1 mg, 0.00080 mmol) and $Zn(AcO)_2\cdot 2H_2O$ (2.6 mg, 0.012 mmol) were mixed in a sealed vessel specifically designed for microwave irradiation, followed by 1.5 mL of $CHCl_3$ and 1.5 mL of toluene. The mixture was stirred inside a microwave reactor at 120 °C for 90 min; the pressure reached 4.7 bar. After cooling, the solvent was removed under vacuum, and the obtained solid was dissolved in 10 mL of $CHCl_3$, placed into a separatory funnel, and washed with 5 mL of H_2O. The organic layer was removed under low pressure to give a purple solid corresponding to **Zn-POctaCor** (1.8 mg, 86%). ^{1}H NMR (500 MHz, chloroform-*d*) δ: 9.41 (s, 8H, H_2), 8.84 (s, 8H, H_6), 8.66 (s, 4H, H_8), 8.34−8.19 (m, 16H, H_{10} + H_{11}), 7.91−7.65 (m, 56H, H_{12} + H_{13} + H_{14} + H_{15} + H_{16} + H_{17} + H_{18}). Due to the low solubility, carbon signals (CH) were detected indirectly via a ^{1}H−^{13}C-HSQC experiment. ^{13}C{^{1}H} NMR (126 MHz, chloroform-*d*) δ: 135.5 (C_6), 132.4 (C_2), 130.4 (C_8), 128.5−125.4 (C_{10} + C_{11} + C_{12} + C_{13} + C_{14} + C_{15} + C_{16} + C_{17} + C_{18}). HRMS (MALDI-TOF) *m/z*: $[M]^+$ calcd for $C_{204}H_{92}N_4Zn$ 2663.6665; found 2663.6528 (13.7 ppm error). UV−vis (toluene): λ 431 (ε = 202 833), 552 (ε = 17 205).

ASSOCIATED CONTENT

Supporting Information

The Supporting Information is available free of charge at https://pubs.acs.org/doi/10.1021/acs.joc.0c00072.

NMR, UV−vis, and MS spectra; complexation measurements; computational methods; optimized geometries;

https://dx.doi.org/10.1021/acs.joc.0c00072
J. Org. Chem. 2020, 85, 4918−4926

noncovalent interactions; synthetic procedures and spectra of compounds (PDF)

AUTHOR INFORMATION

Corresponding Authors

Raúl García-Rodríguez − *GIR MIOMeT, IU CINQUIMA/Química Inorgánica, Facultad de Ciencias, Universidad de Valladolid E-47011 Valladolid, Spain;* orcid.org/0000-0003-0699-3894; Email: raul.garcia.rodriguez@uva.es

Celedonio M. Álvarez − *GIR MIOMeT, IU CINQUIMA/Química Inorgánica, Facultad de Ciencias, Universidad de Valladolid E-47011 Valladolid, Spain;* orcid.org/0000-0003-4431-6501; Email: celedonio.alvarez@uva.es

Authors

Sergio Ferrero − *GIR MIOMeT, IU CINQUIMA/Química Inorgánica, Facultad de Ciencias, Universidad de Valladolid E-47011 Valladolid, Spain*

Héctor Barbero − *GIR MIOMeT, IU CINQUIMA/Química Inorgánica, Facultad de Ciencias, Universidad de Valladolid E-47011 Valladolid, Spain*

Daniel Miguel − *GIR MIOMeT, IU CINQUIMA/Química Inorgánica, Facultad de Ciencias, Universidad de Valladolid E-47011 Valladolid, Spain;* orcid.org/0000-0003-0650-3058

Complete contact information is available at: https://pubs.acs.org/10.1021/acs.joc.0c00072

Notes

The authors declare no competing financial interest.

ACKNOWLEDGMENTS

We thank the Spanish Ministry of Science, Innovation and Universities (MCIU) for funding (project numbers PGC2018-096880-A-I00, MCIU/AEI/FEDER, UE, and PGC2018-099470-B-I00, MCIU/AEI/FEDER, UE). R.G.-R. acknowledges the Spanish MINECO/AEI and the European Union (ESF) for a Ramon y Cajal contract (RYC-2015-19035). H.B. acknowledges the Alfonso Martín Escudero Foundation for a postdoctoral fellowship. We are also grateful to Eduardo Rodriguez-Gutiez for his support with NCIPlot calculations and its implementation in Chimera for visualization purposes.

REFERENCES

(1) (a) Lehn, J.-M. Supramolecular Chemistry—Scope and Perspectives Molecules, Supermolecules, and Molecular Devices (Nobel Lecture). *Angew. Chem., Int. Ed.* **1988**, *27*, 89−112. (b) Lehn, J.-M. From supramolecular chemistry towards constitutional dynamic chemistry and adaptive chemistry. *Chem. Soc. Rev.* **2007**, *36*, 151−160. (c) Lehn, J.-M. Perspectives in Chemistry—Steps towards Complex Matter. *Angew. Chem., Int. Ed.* **2013**, *52*, 2836−2850.

(2) (a) Whitty, A. Cooperativity and biological complexity. *Nat. Chem. Biol.* **2008**, *4*, 435. (b) Reichow, S. L.; Clemens, D. M.; Freites, J. A.; Németh-Cahalan, K. L.; Heyden, M.; Tobias, D. J.; Hall, J. E.; Gonen, T. Allosteric mechanism of water-channel gating by Ca2+−calmodulin. *Nat. Struct. Mol. Biol.* **2013**, *20*, 1085−1092.

(3) (a) Badjić, J. D.; Nelson, A.; Cantrill, S. J.; Turnbull, W. B.; Stoddart, J. F. Multivalency and Cooperativity in Supramolecular Chemistry. *Acc. Chem. Res.* **2005**, *38*, 723−732. (b) Hunter, C. A.; Anderson, H. L. What is Cooperativity? *Angew. Chem., Int. Ed.* **2009**, *48*, 7488−7499. (c) Ercolani, G.; Luca, S. Allosteric, Chelate, and Interannular Cooperativity: A Mise au Point. *Angew. Chem., Int. Ed.* **2011**, *50*, 1762−1768. (d) von Krbek, L. K. S.; Schalley, C. A.; Thordarson, P. Assessing cooperativity in supramolecular systems. *Chem. Soc. Rev.* **2017**, *46*, 2622−2637.

(4) (a) Thordarson, P.; Bijsterveld, E. J. A.; Elemans, J. A. A. W.; Kasák, P.; Nolte, R. J. M.; Rowan, A. E. Highly Negative Homotropic Allosteric Binding of Viologens in a Double-Cavity Porphyrin. *J. Am. Chem. Soc.* **2003**, *125*, 1186−1187. (b) Thordarson, P.; Coumans, R. G. E.; Elemans, J. A. A. W.; Thomassen, P. J.; Visser, J.; Rowan, A. E.; Nolte, R. J. M. Allosterically Driven Multicomponent Assembly. *Angew. Chem., Int. Ed.* **2004**, *43*, 4755−4759. (c) Sato, H.; Tashiro, K.; Shinmori, H.; Osuka, A.; Murata, Y.; Komatsu, K.; Aida, T. Positive Heterotropic Cooperativity for Selective Guest Binding via Electronic Communications through a Fused Zinc Porphyrin Array. *J. Am. Chem. Soc.* **2005**, *127*, 13086−13087. (d) Kremer, C.; Arne, L. Artificial Allosteric Receptors. *Chem. - Eur. J.* **2013**, *19*, 6162−6196.

(5) (a) Shen, Y.; Nakanishi, T. Fullerene assemblies toward photo-energy conversions. *Phys. Chem. Chem. Phys.* **2014**, *16*, 7199−7204. (b) Kirner, S.; Sekita, M.; Guldi, D. M. 25th Anniversary Article: 25 Years of Fullerene Research in Electron Transfer Chemistry. *Adv. Mater.* **2014**, *26*, 1482−1493. (c) Zieleniewska, A.; Lodermeyer, F.; Roth, A.; Guldi, D. M. Fullerenes − how 25 years of charge transfer chemistry have shaped our understanding of (interfacial) interactions. *Chem. Soc. Rev.* **2018**, *47*, 702−714. (d) Collavini, S.; Delgado, J. L. Fullerenes: the stars of photovoltaics. *Sustainable Energy Fuels* **2018**, *2*, 2480−2493.

(6) (a) Diederich, F.; Gómez-López, M. Supramolecular fullerene chemistry. *Chem. Soc. Rev.* **1999**, *28*, 263−277. (b) Pérez, E. M.; Martín, N. Molecular tweezers for fullerenes. *Pure Appl. Chem.* **2010**, *82*, 523−533. (c) Babu, S. S.; Mohwald, H.; Nakanishi, T. Recent progress in morphology control of supramolecular fullerene assemblies and its applications. *Chem. Soc. Rev.* **2010**, *39*, 4021−4035. (d) Canevet, D.; Pérez, E. M.; Martín, N. Wraparound Hosts for Fullerenes: Tailored Macrocycles and Cages. *Angew. Chem., Int. Ed.* **2011**, *50*, 9248−9259. (e) Hardouin−Lerouge, M.; Hudhomme, P.; Sallé, M. Molecular clips and tweezers hosting neutral guests. *Chem. Soc. Rev.* **2011**, *40*, 30−43. (f) Martín, N.; Nierengarten, J. F. *Supramolecular Chemistry of Fullerenes and Carbon Nanotubes*; Wiley-VCH Verlag GmbH: Weinheim, Germany, 2012.

(7) (a) Rabideau, P. W.; Sygula, A. Buckybowls: Polynuclear Aromatic Hydrocarbons Related to the Buckminsterfullerene Surface. *Acc. Chem. Res.* **1996**, *29*, 235−242. (b) Tsefrikas, V. M.; Scott, L. T. Geodesic Polyarenes by Flash Vacuum Pyrolysis. *Chem. Rev.* **2006**, *106*, 4868−4884. (c) Wu, Y.-T.; Siegel, J. S. Aromatic Molecular-Bowl Hydrocarbons: Synthetic Derivatives, Their Structures, and Physical Properties. *Chem. Rev.* **2006**, *106*, 4843−4867. (d) Kawase, T.; Kurata, H. Ball-, Bowl-, and Belt-Shaped Conjugated Systems and Their Complexing Abilities: Exploration of the Concave−Convex $\pi-\pi$ Interaction. *Chem. Rev.* **2006**, *106*, 5250−5273. (e) Sygula, A. Chemistry on a Half-Shell: Synthesis and Derivatization of Buckybowls. *Eur. J. Org. Chem.* **2011**, *2011*, 1611−1625. (f) Rajeshkumar, V.; Marc, C.; Fichou, D.; Stuparu, M. C. Synthesis and Properties of a Buckybowl/Buckyball Dyad. *Synlett* **2016**, *27*, 2101−2104. (g) Li, X.; Kang, F.; Inagaki, M. Buckybowls: Corannulene and Its Derivatives. *Small* **2016**, *12*, 3206−3223. (h) Saito, M.; Shinokubo, H.; Sakurai, H. Figuration of bowl-shaped π-conjugated molecules: properties and functions. *Mater. Chem. Front.* **2018**, *2*, 635−661.

(8) (a) Chen, R.; Lu, R.-Q.; Shi, P.-C.; Cao, X.-Y. Corannulene derivatives for organic electronics: From molecular engineering to applications. *Chin. Chem. Lett.* **2016**, *27*, 1175−1183. (b) Nestoros, E.; Stuparu, M. C. Corannulene: a molecular bowl of carbon with multifaceted properties and diverse applications. *Chem. Commun.* **2018**, *54*, 6503−6519. (c) Haupt, A.; Lentz, D. Tuning the Electron Affinity and Stacking Properties of Corannulene by Introduction of Fluorinated Thioethers. *Chem. - Asian J.* **2018**, *13*, 3022−3026. (d) Gu, X.; Zhang, X.; Ma, H.; Jia, S.; Zhang, P.; Zhao, Y.; Liu, Q.; Wang, J.; Zheng, X.; Lam, J. W. Y.; Ding, D.; Tang, B. Z. Corannulene-Incorporated AIE Nanodots with Highly Suppressed Nonradiative Decay for Boosted Cancer Phototheranostics In Vivo. *Adv. Mater.* **2018**, *30*, No. 1801065. (e) Rice, A. M.; Dolgopolova, E.

A.; Yarbrough, B. J.; Leith, G. A.; Martin, C. R.; Stephenson, K. S.; Heugh, R. A.; Brandt, A. J.; Chen, D. A.; Karakalos, S. G.; Smith, M. D.; Hatzell, K. B.; Pellechia, P. J.; Garashchuk, S.; Shustova, N. B. Stack the Bowls: Tailoring the Electronic Structure of Corannulene-Integrated Crystalline Materials. *Angew. Chem., Int. Ed.* **2018**, *57*, 11310−11315.

(9) (a) Barth, W. E.; Lawton, R. G. Dibenzo[ghi,mno]fluoranthene. *J. Am. Chem. Soc.* **1966**, *88*, 380−381. (b) Lawton, R. G.; Barth, W. E. Synthesis of corannulene. *J. Am. Chem. Soc.* **1971**, *93*, 1730−1745. (c) Seiders, T. J.; Elliott, E. L.; Grube, G. H.; Siegel, J. S. Synthesis of Corannulene and Alkyl Derivatives of Corannulene. *J. Am. Chem. Soc.* **1999**, *121*, 7804−7813. (d) Sygula, A.; Rabideau, P. W. A Practical, Large Scale Synthesis of the Corannulene System. *J. Am. Chem. Soc.* **2000**, *122*, 6323−6324. (e) Butterfield, A. M.; Gilomen, B.; Siegel, J. S. Kilogram-Scale Production of Corannulene. *Org. Process Res. Dev.* **2012**, *16*, 664−676.

(10) (a) Scott, L. T.; Hashemi, M. M.; Bratcher, M. S. Corannulene bowl-to-bowl inversion is rapid at room temperature. *J. Am. Chem. Soc.* **1992**, *114*, 1920−1921. (b) Seiders, T. J.; Baldridge, K. K.; Grube, G. H.; Siegel, J. S. Structure/Energy Correlation of Bowl Depth and Inversion Barrier in Corannulene Derivatives: Combined Experimental and Quantum Mechanical Analysis. *J. Am. Chem. Soc.* **2001**, *123*, 517−525. (c) Nishida, S.; Morita, Y.; Ueda, A.; Kobayashi, T.; Fukui, K.; Ogasawara, K.; Sato, K.; Takui, T.; Nakasuji, K. Curve-Structured Phenalenyl Chemistry: Synthesis, Electronic Structure, and Bowl-Inversion Barrier of a Phenalenyl-Fused Corannulene Anion. *J. Am. Chem. Soc.* **2008**, *130*, 14954−14955. (d) Yanney, M.; Fronczek, F. R.; Henry, W. P.; Beard, D. J.; Sygula, A. Cyclotrimerization of Corannulyne: Steric Hindrance Tunes the Inversion Barriers of Corannulene Bowls. *Eur. J. Org. Chem.* **2011**, *2011*, 6636−6639. (e) Juríček, M.; Strutt, N. L.; Barnes, J. C.; Butterfield, A. M.; Dale, E. J.; Baldridge, K. K.; Stoddart, J. F.; Siegel, J. S. Induced-fit catalysis of corannulene bowl-to-bowl inversion. *Nat. Chem.* **2014**, *6*, 222−228.

(11) (a) Pérez, E. M.; Martín, N. Curves ahead: molecular receptors for fullerenes based on concave-convex complementarity. *Chem. Soc. Rev.* **2008**, *37*, 1512−1519. (b) Pérez, E. M.; Martín, N. π - π interactions in carbon nanostructures. *Chem. Soc. Rev.* **2015**, *44*, 6425−6433. (c) Selmani, S.; Schipper, D. J. π-Concave Hosts for Curved Carbon Nanomaterials. *Chem. - Eur. J.* **2019**, *25*, 6673−6692.

(12) (a) Wu, Y.-L.; Stuparu, M. C.; Boudon, C.; Gisselbrecht, J.-P.; Schweizer, W. B.; Baldridge, K. K.; Siegel, J. S.; Diederich, F. Structural, Optical, and Electrochemical Properties of Three-Dimensional Push−Pull Corannulenes. *J. Org. Chem.* **2012**, *77*, 11014−11026. (b) Stuparu, M. C. Rationally Designed Polymer Hosts of Fullerene. *Angew. Chem., Int. Ed.* **2013**, *52*, 7786−7790. (c) Lu, R.-Q.; Zheng, Y.-Q.; Zhou, Y.-N.; Yan, X.-Y.; Lei, T.; Shi, K.; Zhou, Y.; Pei, J.; Zoppi, L.; Baldridge, K. K.; Siegel, J. S.; Cao, X.-Y. Corannulene derivatives as non-fullerene acceptors in solution-processed bulk heterojunction solar cells. *J. Mater. Chem. A* **2014**, *2*, 20515−20519. (d) Steinauer, A.; Butterfield, A. M.; Linden, A.; Molina-Ontario, A.; Buck, D. C.; Cotta, R. W.; Echegoyen, L.; Baldridge, K. K.; Siegel, J. S. Tunable Photochemical/Redox Properties of (Phenylthio)-ncorannulenes: Application to a Photovoltaic Device. *J. Braz. Chem. Soc.* **2016**, *27*, 1866−1871. (e) Li, J.; Terec, A.; Wang, Y.; Joshi, H.; Lu, Y.; Sun, H.; Stuparu, M. C. π-Conjugated Discrete Oligomers Containing Planar and Nonplanar Aromatic Motifs. *J. Am. Chem. Soc.* **2017**, *139*, 3089−3094. (f) Deng, Y.; Xu, B.; Castro, E.; Fernandez-Delgado, O.; Echegoyen, L.; Baldridge, K. K.; Siegel, J. S. Decakis(arylthio)coranulenes: Transferable Photochemical and Redox Parameters and Photovoltaic Device Performance. *Eur. J. Org. Chem.* **2017**, *2017*, 4338−4342. (g) Barát, V.; Budanović, M.; Halilovic, D.; Huh, J.; Webster, R. D.; Mahadevegowda, S. H.; Stuparu, M. C. A general approach to non-fullerene electron acceptors based on the corannulene motif. *Chem. Commun.* **2019**, *55*, 3113−3116.

(13) (a) Dawe, L. N.; AlHujran, T. A.; Tran, H.-A.; Mercer, J. I.; Jackson, E. A.; Scott, L. T.; Georghiou, P. E. Corannulene and its penta-tert-butyl derivative co-crystallize 1:1 with pristine C60-fullerene. *Chem. Commun.* **2012**, *48*, 5563−5565. (b) Yamada, M.; Ohkubo, K.; Shionoya, M.; Fukuzumi, S. Photoinduced Electron Transfer in a Charge-Transfer Complex Formed between Corannulene and Li+@C60 by Concave−Convex π−π Interactions. *J. Am. Chem. Soc.* **2014**, *136*, 13240−13248.

(14) (a) Sygula, A.; Fronczek, F. R.; Sygula, R.; Rabideau, P. W.; Olmstead, M. M. A Double Concave Hydrocarbon Buckycatcher. *J. Am. Chem. Soc.* **2007**, *129*, 3842−3843. (b) Le, V. H.; Yanney, M.; McGuire, M.; Sygula, A.; Lewis, E. A. Thermodynamics of Host−Guest Interactions between Fullerenes and a Buckycatcher. *J. Phys. Chem. B* **2014**, *118*, 11956−11964.

(15) (a) Yanney, M.; Fronczek, F. R.; Sygula, A. A 2:1 Receptor/C60 Complex as a Nanosized Universal Joint. *Angew. Chem., Int. Ed.* **2015**, *54*, 11153−11156. (b) Abeyratne Kuragama, P. L.; Fronczek, F. R.; Sygula, A. Bis-corannulene Receptors for Fullerenes Based on Klärner's Tethers: Reaching the Affinity Limits. *Org. Lett.* **2015**, *17*, 5292−5295. (c) Kumarasinghe, K. G. U. R.; Fronczek, F. R.; Valle, H. U.; Sygula, A. Bis-corannulenoanthracene: An Angularly Fused Pentacene as a Precursor for Barrelene-Tethered Receptors for Fullerenes. *Org. Lett.* **2016**, *18*, 3054−3057.

(16) (a) Álvarez, C. M.; García-Escudero, L. A.; García-Rodríguez, R.; Martín-Álvarez, J. M.; Miguel, D.; Rayón, V. M. Enhanced association for C70 over C60 with a metal complex with corannulene derivate ligands. *Dalton Trans.* **2014**, *43*, 15693−15696. (b) Yang, D.-C.; Li, M.; Chen, C.-F. A bis-corannulene based molecular tweezer with highly sensitive and selective complexation of C70 over C60. *Chem. Commun.* **2017**, *53*, 9336−9339.

(17) (a) Yanney, M.; Sygula, A. Tridental molecular clip with corannulene pincers: is three better than two? *Tetrahedron Lett.* **2013**, *54*, 2604−2607. (b) Álvarez, C. M.; Aullón, G.; Barbero, H.; García-Escudero, L. A.; Martínez-Pérez, C.; Martín-Álvarez, J. M.; Miguel, D. Assembling Nonplanar Polyaromatic Units by Click Chemistry. Study of Multicorannulene Systems as Host for Fullerenes. *Org. Lett.* **2015**, *17*, 2578−2581. (c) Álvarez, C. M.; Barbero, H.; Ferrero, S. Preparation of a Corannulene-functionalized Hexahelicene by Copper(I)-catalyzed Alkyne-azide Cycloaddition of Nonplanar Polyaromatic Units. *J. Visualized Exp.* **2016**, *115*, No. e53954.

(18) (a) Barbero, H.; Ferrero, S.; Álvarez-Miguel, L.; Gómez-Iglesias, P.; Miguel, D.; Álvarez, C. M. Affinity modulation of photoresponsive hosts for fullerenes: light-gated corannulene tweezers. *Chem. Commun.* **2016**, *52*, 12964−12967. (b) Álvarez, C. M.; Barbero, H.; Ferrero, S.; Miguel, D. Synergistic Effect of Tetraaryl Porphyrins Containing Corannulene and Other Polycyclic Aromatic Fragments as Hosts for Fullerenes. Impact of C60 in a Statistically Distributed Mixture of Atropisomers. *J. Org. Chem.* **2016**, *81*, 6081−6086. (c) García-Calvo, V.; Cuevas, J. V.; Barbero, H.; Ferrero, S.; Álvarez, C. M.; González, J. A.; Díaz de Greñu, B.; García-Calvo, J.; Torroba, T. Synthesis of a Tetracorannulene-perylenediimide That Acts as a Selective Receptor for C60 over C70. *Org. Lett.* **2019**, *21*, 5803−5807.

(19) (a) Boyd, P. D. W.; Hodgson, M. C.; Rickard, C. E. F.; Oliver, A. G.; Chaker, L.; Brothers, P. J.; Bolskar, R. D.; Tham, F. S.; Reed, C. A. Selective Supramolecular Porphyrin/Fullerene Interactions1. *J. Am. Chem. Soc.* **1999**, *121*, 10487−10495. (b) Boyd, P. D. W.; Reed, C. A. Fullerene−Porphyrin Constructs. *Acc. Chem. Res.* **2005**, *38*, 235−242. (c) Tashiro, K.; Aida, T. Metalloporphyrin hosts for supramolecular chemistry of fullerenes. *Chem. Soc. Rev.* **2007**, *36*, 189−197. (d) Saegusa, Y.; Ishizuka, T.; Kojima, T.; Mori, S.; Kawano, M.; Kojima, T. Supramolecular Interaction of Fullerenes with a Curved π-Surface of a Monomeric Quadruply Ring-Fused Porphyrin. *Chem. - Eur. J.* **2015**, *21*, 5302−5306. (e) Bromby, A. D.; Hogan, D. T.; Sutherland, T. C. Core expanded, 21,23-dithiadiacenaphtho[1,2-c]porphyrin interactions with [60]fullerene. *New J. Chem.* **2017**, *41*, 4802−4805. (f) Yamada, M.; Murakami, G.; Kobayashi, S.; Maeda, Y. Enhancing solution-phase supramolecular interactions between monomeric porphyrins and [60]fullerene by simple chemical modification. *Tetrahedron Lett.* **2017**, *58*, 4514−4518.

(20) Ferrero, S.; Barbero, H.; Miguel, D.; García-Rodríguez, R.; Álvarez, C. M. Dual-Tweezer Behavior of an Octapodal Pyrene

https://dx.doi.org/10.1021/acs.joc.0c00072
J. Org. Chem. 2020, 85, 4918−4926

Porphyrin-Based System as a Host for Fullerenes. *J. Org. Chem.* **2019**, *84*, 6183−6190.
(21) (a) Kappe, C. O. Controlled Microwave Heating in Modern Organic Synthesis. *Angew. Chem., Int. Ed.* **2004**, *43*, 6250−6284. (b) Sharma, N.; K. Sharma, U.; Van der Eycken, E. V. *Green Techniques for Organic Synthesis and Medicinal Chemistry*; Zhang, W.; Cue, B. W., Eds.; Wiley: New York, 2018; pp 441−468.
(22) (a) Sygula, A.; Saebø, S. π-π Stacking of curved carbon networks: The corannulene dimer. *Int. J. Quantum Chem.* **2009**, *109*, 65−72. (b) Mück-Lichtenfeld, C.; Grimme, S.; Kobryn, L.; Sygula, A. Inclusion complexes of buckycatcher with C60 and C70. *Phys. Chem. Chem. Phys.* **2010**, *12*, 7091−7097. (c) Janowski, T.; Pulay, P.; Sasith Karunarathna, A. A.; Sygula, A.; Saebø, S. Convex−concave stacking of curved conjugated networks: Benchmark calculations on the corannulene dimer. *Chem. Phys. Lett.* **2011**, *512*, 155−160. (d) Topolinski, B.; Schmidt, B. M.; Kathan, M.; Troyanov, S. I.; Lentz, D. Corannulenylferrocenes: towards a 1D, non-covalent metal-organic nanowire. *Chem. Commun.* **2012**, *48*, 6298−6300. (e) Sygula, A.; Yanney, M.; Henry, W. P.; Fronczek, F. R.; Zabula, A. V.; Petrukhina, M. A. Inclusion Complexes and Solvates of Buckycatcher, a Versatile Molecular Host with Two Corannulene Pincers. *Cryst. Growth Des.* **2014**, *14*, 2633−2639.
(23) (a) Ditchfield, R.; Hehre, W. J.; Pople, J. A. Self-Consistent Molecular-Orbital Methods. IX. An Extended Gaussian-Type Basis for Molecular-Orbital Studies of Organic Molecules. *J. Chem. Phys.* **1971**, *54*, 724−728. (b) Hehre, W. J.; Ditchfield, R.; Pople, J. A. Self—Consistent Molecular Orbital Methods. XII. Further Extensions of Gaussian—Type Basis Sets for Use in Molecular Orbital Studies of Organic Molecules. *J. Chem. Phys.* **1972**, *56*, 2257−2261. (c) Francl, M. M.; Pietro, W. J.; Hehre, W. J.; Binkley, J. S.; Gordon, M. S.; DeFrees, D. J.; Pople, J. A. Self-consistent molecular orbital methods. XXIII A polarization-type basis set for second-row elements. *J. Chem. Phys.* **1982**, *77*, 3654−3665. (d) Grimme, S. Semiempirical GGA-type density functional constructed with a long-range dispersion correction. *J. Comput. Chem.* **2006**, *27*, 1787−1799. (e) Grimme, S.; Ehrlich, S.; Goerigk, L. Effect of the damping function in dispersion corrected density functional theory. *J. Comput. Chem.* **2011**, *32*, 1456−1465.
(24) (a) Pons, M.; Millet, O. Dynamic NMR studies of supramolecular complexes. *Prog. Nucl. Magn. Reson. Spectrosc.* **2001**, *38*, 267−324. (b) Bain, A. D. Chemical exchange in NMR. *Prog. Nucl. Magn. Reson. Spectrosc.* **2003**, *43*, 63−103. (c) Kleckner, I. R.; Foster, M. P. An introduction to NMR-based approaches for measuring protein dynamics. *Biochim. Biophys. Acta, Proteins Proteomics* **2011**, *1814*, 942−968.
(25) (a) Blackburn, M. N.; Schachman, H. K. Allosteric regulation of aspartate transcarbamoylase. Effect of active site ligands on the reactivity of sulfhydryl groups of the regulatory subunits. *Biochemistry* **1977**, *16*, 5084−5091. (b) Endrizzi, J. A.; Beernink, P. T.; Alber, T.; Schachman, H. K. Binding of bisubstrate analog promotes large structural changes in the unregulated catalytic trimer of aspartate transcarbamoylase: Implications for allosteric regulation. *Proc. Natl. Acad. Sci. U.S.A.* **2000**, *97*, 5077−5082.
(26) (a) Ackers, G. K.; Doyle, M. L.; Myers, D.; Daugherty, M. A. Molecular code for cooperativity in hemoglobin. *Science* **1992**, *255*, 54. (b) Eaton, W. A.; Henry, E. R.; Hofrichter, J.; Mozzarelli, A. Is cooperative oxygen binding by hemoglobin really understood? *Nat. Struct. Biol.* **1999**, *6*, 351−358. (c) Lukin, J. A.; Ho, C. The Structure−Function Relationship of Hemoglobin in Solution at Atomic Resolution. *Chem. Rev.* **2004**, *104*, 1219−1230. (d) Nagatomo, S.; Nagai, M.; Kitagawa, T. A New Way To Understand Quaternary Structure Changes of Hemoglobin upon Ligand Binding On the Basis of UV-Resonance Raman Evaluation of Intersubunit Interactions. *J. Am. Chem. Soc.* **2011**, *133*, 10101−10110.
(27) (a) Johnson, E. R.; Keinan, S.; Mori-Sánchez, P.; Contreras-García, J.; Cohen, A. J.; Yang, W. Revealing Noncovalent Interactions. *J. Am. Chem. Soc.* **2010**, *132*, 6498−6506. (b) Contreras-García, J.; Johnson, E. R.; Keinan, S.; Chaudret, R.; Piquemal, J.-P.; Beratan, D. N.; Yang, W. NCIPLOT: A Program for Plotting Noncovalent Interaction Regions. *J. Chem. Theory Comput.* **2011**, *7*, 625−632.
(28) (a) Lemon, C. M.; Brothers, P. J.; Boitrel, B. Porphyrin complexes of the period 6 main group and late transition metals. *Dalton Trans.* **2011**, *40*, 6591−6609. (b) Kadish, K. M.; Smith, K. M.; Guilard, R. *Handbook of Porphyrin Science*; World Scientific Publishing Company, 2012; Vol. *21*−*25*. (c) Valicsek, Z.; Horváth, O. Application of the electronic spectra of porphyrins for analytical purposes: The effects of metal ions and structural distortions. *Microchem. J.* **2013**, *107*, 47−62. (d) Senge, M. O.; MacGowan, S. A.; O'Brien, J. M. Conformational control of cofactors in nature - the influence of protein-induced macrocycle distortion on the biological function of tetrapyrroles. *Chem. Commun.* **2015**, *51*, 17031−17063.
(29) (a) Armarego, W. L. F.; Chai, C. L. L. *Purification of Laboratory Chemicals*, 6th ed.; Butterworth-Heinemann: London, 2009. (b) Williams, D. B. G.; Lawton, M. Drying of Organic Solvents: Quantitative Evaluation of the Efficiency of Several Desiccants. *J. Org. Chem.* **2010**, *75*, 8351−8354.
(30) (a) Wegner, H. A.; Scott, L. T.; de Meijere, A. A New Suzuki−Heck-Type Coupling Cascade: Indeno[1,2,3]-Annelation of Polycyclic Aromatic Hydrocarbons. *J. Org. Chem.* **2003**, *68*, 883−887. (b) Da Ros, S.; Linden, A.; Baldridge, K. K.; Siegel, J. S. Boronic esters of corannulene: potential building blocks toward icosahedral supramolecules. *Org. Chem. Front.* **2015**, *2*, 626−633.

https://dx.doi.org/10.1021/acs.joc.0c00072
J. Org. Chem. 2020, 85, 4918−4926